ZAMORNA ČVRSTOĆA ZAVARA S OBZIROM NA ZAOSTALA NAPREZANJA

FATIGUE STRENGTH OF WELDS IN THE VIEW OF RESIDUAL STRESSES

V. GLIHA[1)], **P. MARUSCHAK**[2)], **O. YASNIY**[2)], **R. BISCHAK**[2)], **I. SAMARDŽIĆ**[3)], **T. VUHERER**[1)]

Ključne riječi: zamorna čvrstoća zavara, zaostala naprezanja

Keywords: fatigue strength of welds, residual stresses

Sažetak: Zamorna čvrstoća metala kao i djelova zavara na metalima zavisi od tvrdoće, veličine greški i veličine zrna. Zamorna čvrstoća zavisi i od razine lokalnih zaostalih naprezanja. Eksperimentalno je utvrđen utjecaj razine zaostalih naprezanja i veličine zrna na zamornu čvrstoću zavara realne kvalitete koristeći uzorke materijala, koji su pripremljeni na simulatoru toplotnog ciklusa i u laboratorijskoj peći. Ocjenjene su i komentirane varijacije tvrdoće u zavarima i plakaturi.

Abstract: The fatigue strength of metals as well as of weld joint regions in metals depends on the hardness, the size of defects and the size of grains. The fatigue strength depends on the local welding residual stress level, too. The effects of residual stresses level and grain size on the fatigue strength of real quality weld materials were experimentally determined using samples prepared on a thermal cycle simulator and a laboratory furnace. Variations of hardness in welds and clad materials were assessed and discussed.

[1)] University of Maribor, Faculty of Mechanical Engineering, Slovenia
[2)] Ternopil Ivan Pul'uj State Technical University, Ukraine
[3)] Josip Juraj Strossmayer University of Osijek, Faculty of Mechanical Engineering, Slavonski Brod

1. INTRODUCTION

Cracks often initiate from microstructurally small defects. Much smaller cracks than the most important microstructural units of metals have no influence on the fatigue limit. Effect of other defects of the same size is similar. Initiated cracks propagate fast at the beginning. When approaching micro structural obstacles they decelerate and can stop. Those cracks are non-propagating. Kitagawa-Takahashy diagram describes the fatigue limit of metals with non-propagating cracks [1].

In the vicinity of welds large thermal stress gradients spring up during welding and cause welding RS appearance. The type and level of RS are crucial for the fatigue strength of welds in the as-welded condition. Formation of the HAZ is the next important consequence of welding. Material adjacent to the fusion line is namely heated almost to the melting point. The result is an extensive grain growth.

Butt-welds are the strongest welds. The fatigue strength of butt-welds is affected by their shape. Stress concentration is the highest at the weld toes. Toes coincide with the location of CGHAZ. Hardness of CGHAZ depends upon of chemical composition, initial state of BM and applied welding parameters.

Defects are always present in metals due to the way of processing. Weld defects in the WM and HAZ appear mainly due to the nature of welding process. Defects that are smaller than the threshold sensitivity of the NDE method cannot be detected. Local R-ratio has significant role in the fatigue limit of welds.

The results are discussed in this article in the light of fatigue behaviour of specimens with stress concentration like at the weld toe. Specimens' surface was prepared either smooth or with surface defect. Two types of small artificial surface defects were used in the experimental work; drilled holes and Vickers indentations. Specimens were made from steel with different average grain size. The result o microstructure preparation on thermal-cycle simulator and using water quenching is different RS level.

2. FATIGUE LIMIT OF METALS WITH SMALL DEFECTS

Cracks initiation at the weld toe is important for the fatigue strength of welds. Small weld defects as different inclusions, scratches or cracks are often found at the weld toes. Even sharp transition from the weld reinforcement to the BM should be small defect. Fatigue cracks in butt-welds usually initiate in the CGHAZ, i.e. in the coarse-grain steel. Small surface defects are also present there [2].

Murakami and co-workers treated the influence of various small defects in the same way as cracks using LEFM [3–5]. The parameter reflecting the effect of small defects on the fatigue limit of metallic materials is square root of the defect $\sqrt{\text{area}}$. The fatigue limit, σ_w, is predicted using only two parameters; defect size and material hardness.

$$\sigma_w = \frac{1.43\,(\text{HV} + 120)}{\left(\sqrt{\text{area}}\right)^{\frac{1}{6}}} \tag{1}$$

σ_w is expressed in MPa, HV in Vickers hardness number and $\sqrt{\text{area}}$ in μm.

Small weld defects in metals can be modelled artificially. As small surface defects drilled small holes and Vickers indentation are used. Indenting with the Vickers pyramid is very convenient. Load on the pyramid is adjusted according to the hardness and needed indentation

size [6, 7].

Problem with use of artificial weld defects is appearance of the local RS. Those stresses are result of irreversible material deformation when manufacturing defects. In order to evaluate the effects of small defect to the fatigue limit, RS should be omitted. They can be global and local. Electro-etching is usually used to remove surface stratum with the highest RS without any plastic deformation. In such a way, local and global surface RS are lowered. Unfortunately, local RS lowering is close linked with the defect's shape and size change. When global RS are present it is not possible to annul only local RS.

Some effects of local RS caused by the defects manufacturing were already discussed elsewhere [8, 9]. It was also shown how to carry out two steps heat treatment in order to obtain small artificial defects on the specimens with microstructure of martensite without presence of local RS.

3. EXPERIMENTAL WORK AND RESULTS

Chemical composition of the used nickel-molybdenum steel is shown in Table 1.

Table 1: Chemical composition of the nickel-molybdenum steel

C	Si	Mn	P	S	Cr	Ni	Mo	Cu	Al
mass %									
0.18	0.22	0.43	0.012	0.028	1.56	1.48	0.28	0.15	0.023

HAZ microstructure was prepared on pieces of the steel using thermal cycle simulator and two different heat treatments in furnace. Thermal regime during the single-cycle simulation on a thermal cycle simulator is shown in Figure 1. Peak temperature T_p was on the level 1300 °C while cooling time $\Delta t_{8/5}$ was round 5 s. The result was martensitic microstructure formation characterised for the CGHAZ, the region found close to the weld fusion line.

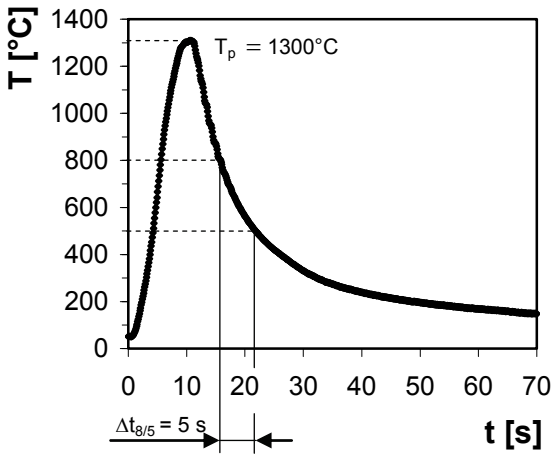

Figure 1: Temperature lapse on pieces of steel characterised by peak temperature (T_p) and cooling time ($\Delta t_{8/5}$) that result is in CGHAZ formation with the microstructure of martensite

Our aim in modelling single-step heat treatment in furnace was to obtain the same microstructure as in the case of using thermal cycle simulator. The procedure is shown in Figure 2a. Two-step heat treatment in furnace was used to obtain double-cycle HAZ microstructure. It is shown in Figure 2b. The result of double-cycle simulation in furnace is re-fined martensitic

HAZ microstructure also characterised for the region found close to the fusion line.

At the beginning of both heat treatments a 3-hours-coarse-grain annealing at 1100 °C was performed on pieces of steel in the furnace: a) In order to prepare CGHAZ microstructure temperature in the furnace was lowered to 870 °C and then water quenched. The result was coarse-grain microstructure of martensite very likely to that formed at the weld toe in the case of single pass "cold welding". B) In order to prepare re-fined HAZ microstructure pieces of steel were after annealing cooled in the water. In the next step of heat treatment re-austenitised steel was water quenched from 870 °C. The result was re-fined microstructure of martensite very likely to that formed at the weld toe in the case of double-pass "cold welding" when tempering weld-passes are applied to the top layer.

Compressive surface global RS are result of cylindrical steel pieces water quenching. They were assessed by the hole-drilling method to be round –300 MPa [10]. In contrast, heat conveying from steel pieces by means of water cooled grips during welding simulation on the weld thermal-cycle simulator results in tensile surface global RS. It was not possible to quantify the level of RS at the bottom of the circumferential notched specimens using hole-drilling method, but they are tensile.

Microstructures of martensite prepared by temperature lapses shown in Figures 1 and 2 are presented in Figure 3. They are named steels with microstructure MS-a, MS-b and MS-c.

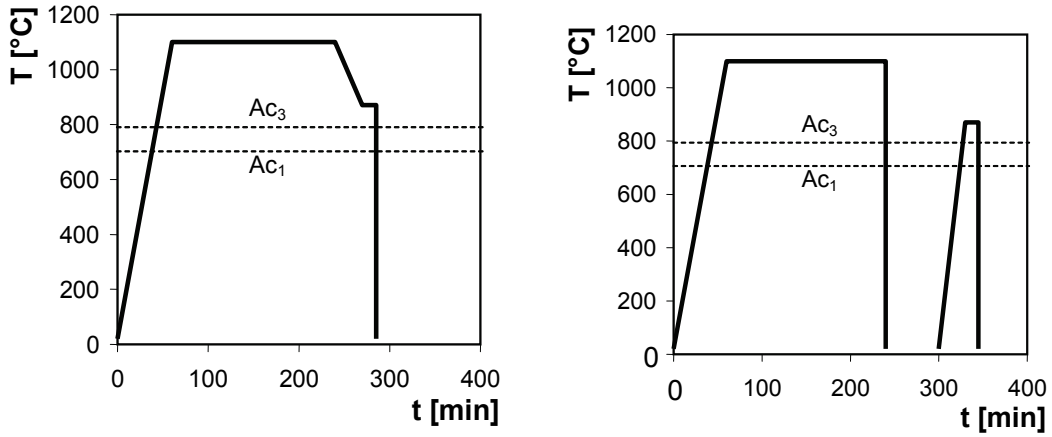

a b

Figure 2: a) Heat treatments in furnace: simulation of CGHAZ microstructure of martensite; b) Simulation of re-fined HAZ microstructure of martensite

Bend-specimens were machined from samples of those steels. They were circularly notched in the mid-length. The shape and size of those specimens are shown in Figure 4. Stress concentration factor in bending is 1.74 [11].

After the simulations small artificial surface defect was prepared at the bottom of the notch. They were drilled holes and Vickers indentations. The appearance of both defects is shown in Figure 5.

Smooth and defected specimens were bend-loaded on a rotary bending machine at room temperature in the moment-control mode. Frequency of the loading was 100 HZ. Stress rate was $R = -1$. The defect size parameter was the same for both defects $\sqrt{\text{area}} \cong 54$ μm.

Hardness of martensitic steels MS-a, MS-b and MS-c is round 440 HV [10]. Average grain size of the steels MS-a and MS-b is 200 μm while of the steel MS-c 20-30 μm [10]. Surface RS in the samples of steels MS-a are tensile. Exact level of those stresses is not known. On samples

of steel MS-b and MS-c surface RS were experimentally determined. They are round –300 MPa [10].

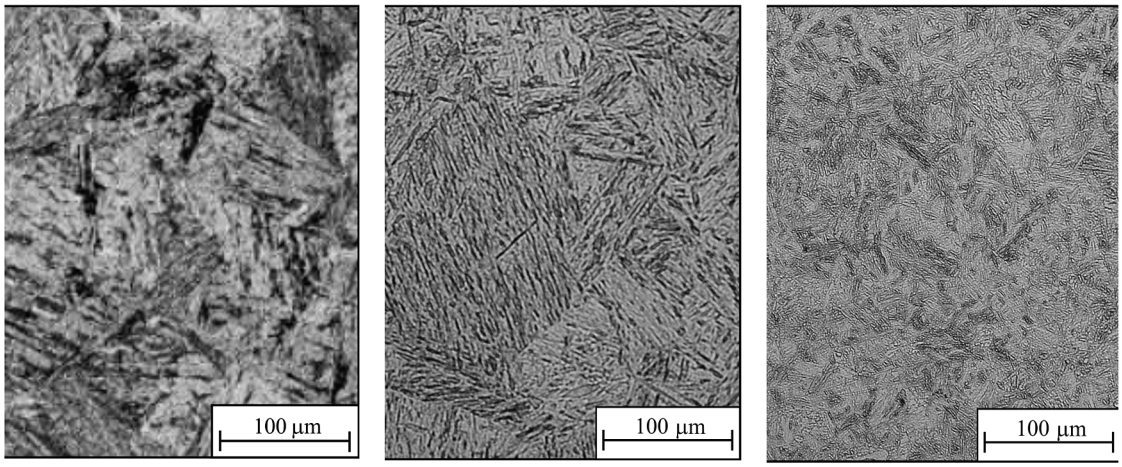

a b c

Figure 3: a) Martensitic coarse-grain microstructure, MS-a, prepared by weld thermal cycle; b) Martensitic coarse-grain microstructure, MS-b, prepared by single-step thermal treatment in furnace; c) Re-fined martensitic microstructure, MS-c, prepared by two-step thermal treatment in furnace

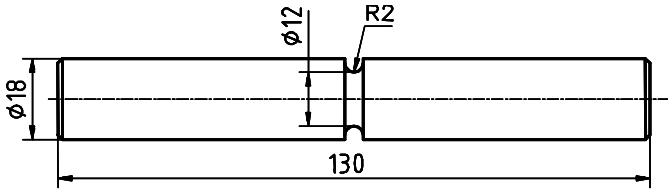

Figure 4: Geometry of rotary bend-specimen

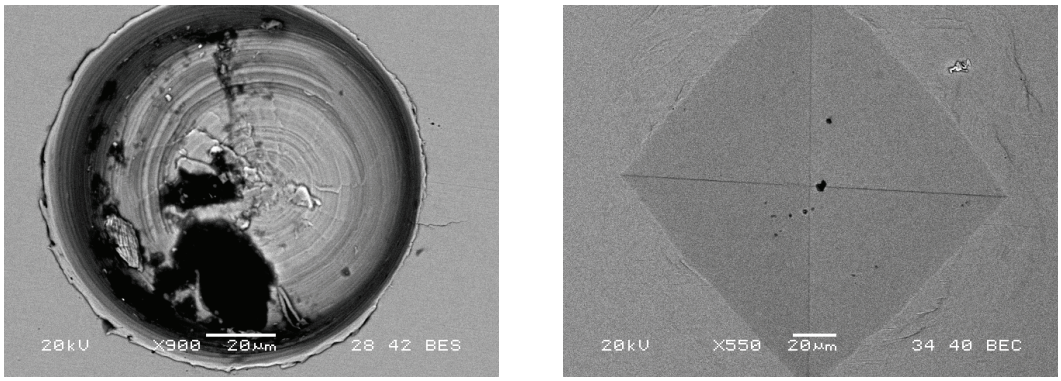

a b

Figure 5: Artificial surface defects: a) Drilled hole with diameter 90 µm and depth 45 µm; b) Indentation made by Vickers pyramid with the diagonal 200 µm

The result of testing was bending fatigue strength of specimens manufactured from steels MS-a, MS-b and MS-c with and without small defect on the surface. The average grain size of studied steels was not the same. The fatigue strength of specimens is determined in two different global RS conditions. The results are shown in Table 2.

Table 2: The bending fatigue strength of steels MS-a, MS-b and MS-c in different conditions

Steel	MS-a	MS-b	MS-c	MS-a	MS-b	MS-c
Grain size, μm	200	200	20-30	200	200	20-30
RS, MPa	tensile	≅ –300	≅–300	tensile	≅ –300	≅ –300
Surface	smooth	smooth	smooth	defected	defected	defected
Fatigue strength, MPa	≅ 330	≅ 537	≅ 760	≅ 330	–	664-678

At the stress level a little bit lower than the fatigue limit of steels small cracks appear. They emerge either at the surface of smooth specimen (Figure 6) or from defects (Figure 7). They begin to propagate, but cracks propagation stop. Those cracks that have been first initiated and then propagated to the certain size belong to non-propagating cracks.

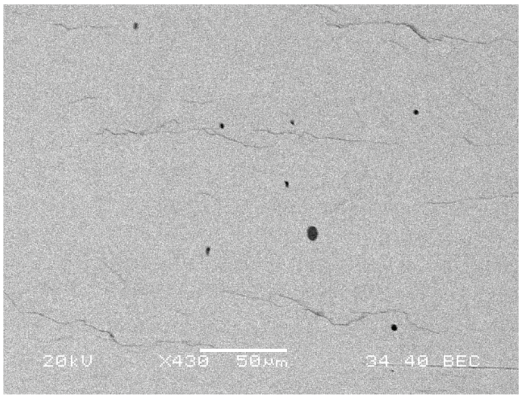

Figure 6: Stable cracks initiated on the specimen without surface defects

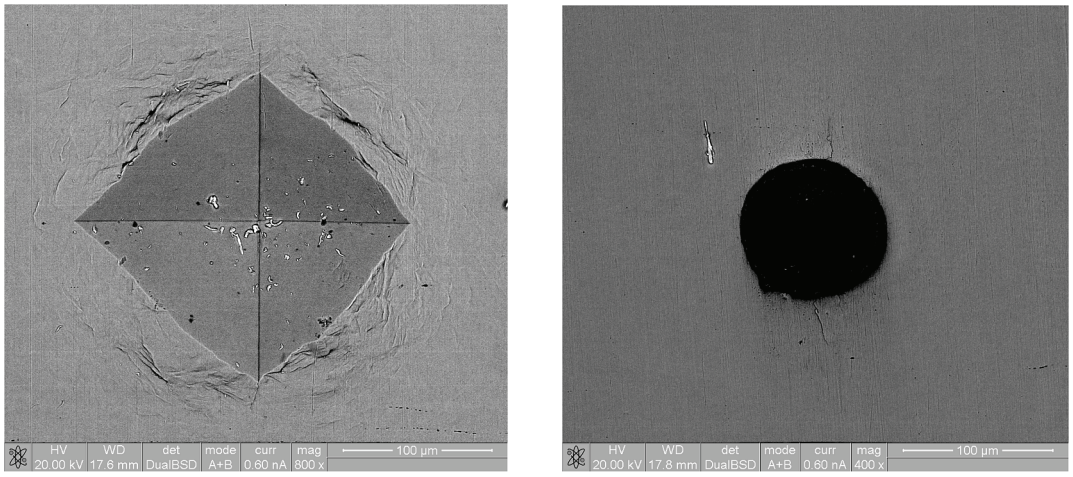

a b

Figure 7: Stable cracks initiated on the defected specimen. Small artificial surface defects: a) Vickers indentation; b) Drilled hole

The effect of local RS caused by manufacturing of defects, i.e. drilling holes and indenting with the Vickers pyramid with equal parameter $\sqrt{\text{area}} \cong 54$ μm is up to 13 % [8-10].

A 12 mm tick but-welded coupon in the structural steel plate grade HT 50 was prepared to assess global RS level caused by welding and weld repairing. Chemical composition and basic

mechanical properties of the steel are shown in Table 3. Steel was in the quenched and tempered condition. A 3-weld-pass butt-weld was made by submerged arc welding (SAW) using flux-cored wire Filtub 128 and flux FB TT. Net heat-input was 17-18 KJ/cm. Preheating was not applied. Inter-pass temperature was kept 70 °C. The chemical composition and the basic mechanical properties of the consumable are shown in Table 3.

The repair weld was made by grooving the weld to the depth round 7 mm in length 100 mm and filling it by shielded metal arc welding (SMAW) using stick electrode EVB NiMo with basic coating without preheating. Net heat-input by welding was 9 KJ/cm. Inter-pass temperature was kept 70 °C. The chemical composition and the basic mechanical properties of consumable are shown in Table 3.

Table 3: Chemical composition and properties of the steel and welding consumables

	C	Si	Mn	P	S	Cr	Ni	Mo	$R_{p0.2}$	R_m	$CVN_{-40\,°C}$
Material	mass %								MPa	MPa	J
BM	0,06	0,34	0,41	0,010	0,004	0,73	0,27	0,036	>490	520–670	118/78
Wire	0,05	0,20	1,40	-	-	-	1,20	0,40	>550	630–730	100
Electrode	0,06	0,40	0,90	-	-	-	1,10	0,35	>510	580–710	47

Additionally a piece of roll from continuous casting machine was analysed as regard hardness across the cladding made by welding. The chemical composition and the basic mechanical properties of both steels are shown in Table 4.

Table 4: Chemical composition of steels 35G2 and 18Kh11MNFB

	C	Si	Ni	Cu	Cr	Mn	Mo	V	CVN, J/sm^2	$R_{p0.2}$	R_m
35G2 – base m.	0,35	0,25	0,3	0,3	0,3	1,4	-	-	34	275	530
18Kh11MNFB – clad material	0,18	0,6	1,0	-	11	1,0	0,7	0,2	60	600	750

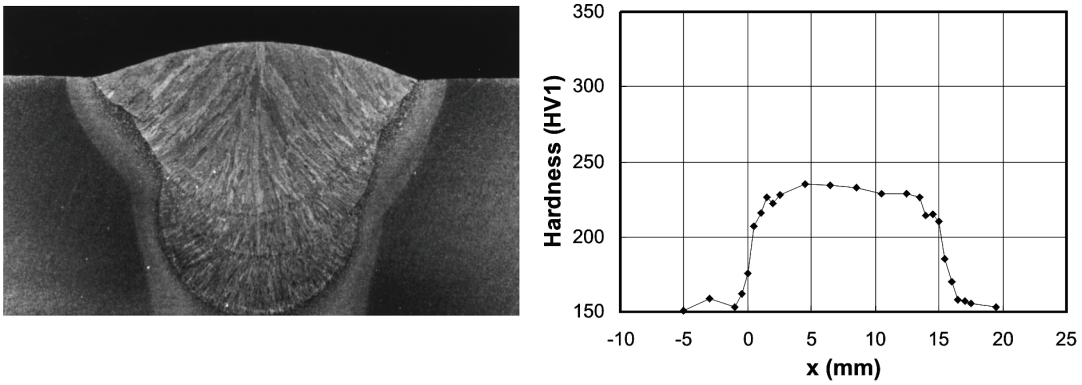

a b

Figure 8: a) Cross-section of the weld; b) Hardness across the weld

Photograph of the primary (not repaired) weld cross-section and variations in hardness across the last weld-pass in the as-welded condition are shown in Figure 8. Photograph of the clad material where cladding is made by welding and variations in hardness across the clad material are shown in Figure 9. We can noticed changes in hardness from 50 % to more than 100 %.

Welding RS were measured in the as-welded condition on primary weld and repaired weld. The hole-drilling method was used [12]. Weld reinforcement was carefully removed and strain-gauge rosettes attached. The results of surface welding RS measurement in the middle of the weld in the transverse direction are shown in Figure 10.

The level of RS in repaired weld is much higher than that measured in the primary weld. Stresses in the middle of the primary weld are tensile (between +10 and +60 MPa). Stresses in the middle of the weld after repair are tensile (between +20 and +180 MPa).

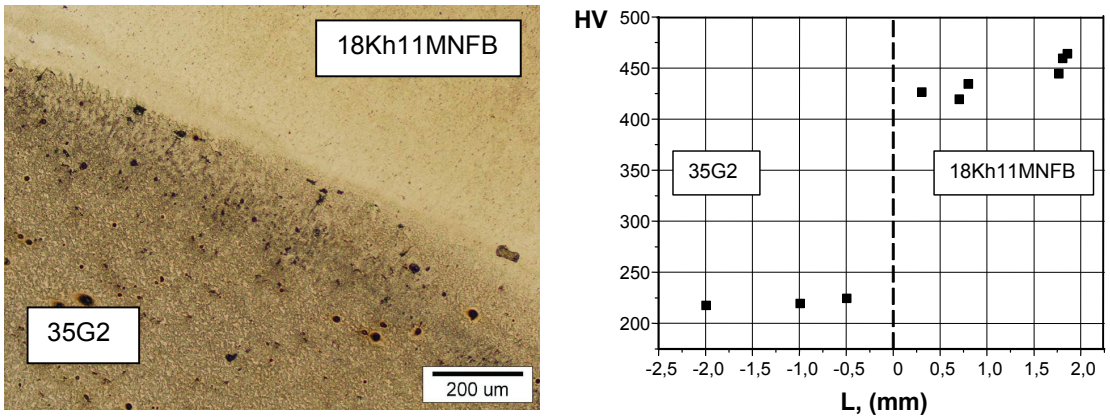

a b

Figure 9: a) Welded cladding appearance; b) Hardness across the base and clad materials

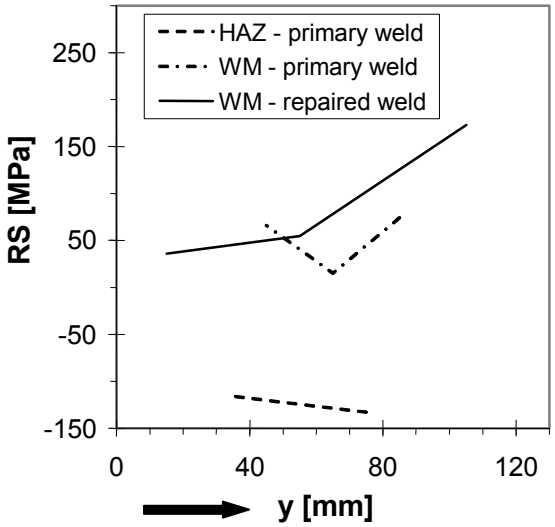

Figure 10: Transverse welding RS along the weld in the primary weld and repaired weld

4. DISCUSSION WITH CONCLUSIONS

It was proven in the past by experiments that the fatigue limit of polycrystalline metallic materials as well as the threshold stress intensity factor that defines condition for the development of macroscopic crack from small defects depends upon only two variables; defect size and material hardness [5]. Miller [13] pointed out the responsibility of microstructural obstacles for existence of non-propagating cracks at the stress level equal to fatigue limit. The

most important obstacles link with the biggest microstructural units of metals, i.e. grains, colonies of pearlite in steels with microstructure of ferrite and pearlite, domains with harder microstructural constituent in steels with duplex microstructure, etc. If we take into account only grains distances between grain boundaries should be considered. They are more sparsely distributed in space in the coarse grain microstructure than in the fine grain microstructure.

The fatigue limit of polycrystalline metals like steel found at the weld toe on welds in the carbon steels as CGHAZ and re-fined HAZ is not only two parameters dependent. Defects size and material hardness in the present article were namely constant, but nevertheless we registered differences in the experimentally determined fatigue limit of the studied steels. It seems that grain size and global RS level in real welds are by far not less important than size of defects and hardness of welds. This is of great importance for load carrying capacity of welds under fatigue loading.

So, the experimental results listed in Table 2 are surface quality, grain size and global RS level dependent. Let's look deeper on those results in relation to the single variable when other two variables are constant. The results are three very simple diagrams. They express the fatigue limit dependence upon the surface quality (SQ), the grain size (GS) and the RS level (RSL). The diagrams are shown in Figure 11. Such an interpretation of the results actually explains some very important facts in relation to fatigue strength of welds or cladding made by welding in which we assessed change of welding RS and weld hardness.

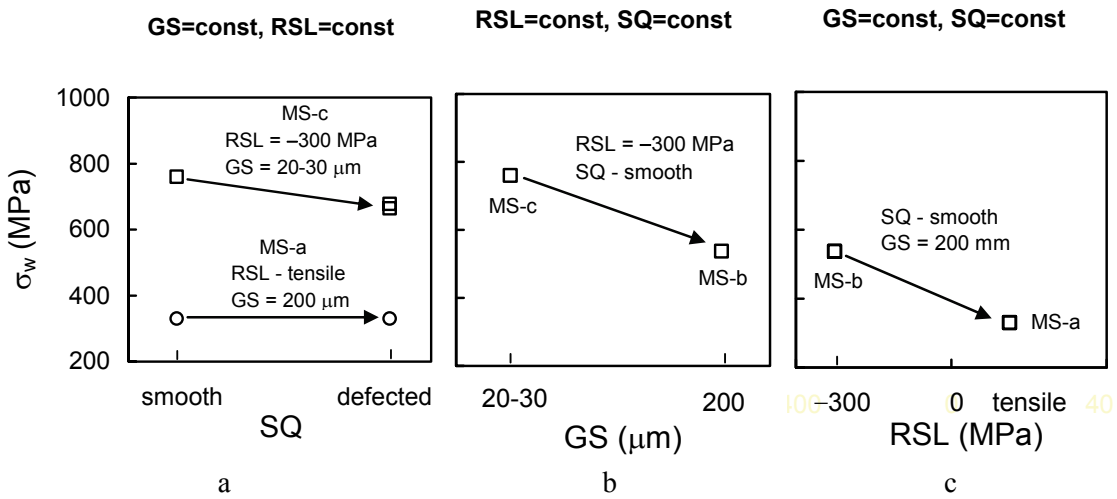

Figure 11: Influential variables to the fatigue limit of studied steels: a) Surface quality-SQ; b) Grain size-GS; c) Residual stress level-RSL

As it is expected, the fatigue limit of steels measured on the surface of defected specimens does not exceed the fatigue limit that is determined on smooth specimens. The size of the defect parameter $\sqrt{\text{area}}$ in the steel MS-c (54 μm) is comparable with the average grain size of steel MS-c (20-30 μm) while the same size of the defect parameter $\sqrt{\text{area}}$ in the steel MS-a is much smaller than the average grain size of steel MS-a (200 μm).

If a direct consequence of repair welding were new inclusions, bigger scratches or cracks or sharper transitions from the repair weld to the base (BM or WM) the fatigue strength of repaired weld would lower in relation to the primary weld.

In the case of smooth specimens manufactured from steels MS-b and MS-c RS level is the same (–300 MPa) but the fatigue limit of the steel MS-c is higher than the fatigue limit of the steel MS-b.

The reason is re-fined grain in the steel MS-c (20-30 μm) in comparison with coarse grain in the steel MS-b (200 μm).

Weld repairing can enlarge grains. Deposition of a new weld-pass is linked with the additional heat input to the material. The consequence is some grain growth.

In the case of smooth specimens manufactured from steels MS-a and MS-b grain size is the same (200 μm) but the fatigue limit of the steel MS-a is much lower than the fatigue limit of the steel MS-b. The reason are tensile RS in the former steel in comparison to compressive ones in the last steel (–300 MPa).

Welding RS change due to repair welding. As shown in Figure 10a RS in the primary weld measured in the WM were lower than RS in the repaired weld measured also in the WM. The main reason for an enhancement of RS is higher restraint. The highest RS in the repair weld were registered at the end of weld repair made by welding.

As seen in Figure 8b and 9b, weld and cladding hardness can be drastically different than the thermally uninfluenced BM hardness. The main reason can be a lower heat input demanded because of less space in the grooved part of weld, use of a harder or softer electrode, too low preheating used etc.

Hardening of weld materials caused by repair welding has effect upon the fatigue strength of welds. It leads to its increase. In contrast, higher welding RS caused by repair welding lead to drastic fatigue strength reduction of welds. Grain growth during repair welding makes material of weld domains less sensitive to small defects. Lower cladding hardness is inconvenient in respect of crack initiation from small defects at the surface of clad rolls.

5. REFERENCES

[1] Kitagawa, H., Takahashi, S. Applicability of Fracture Mechanics to Very Small Cracks or the Cracks in the Early Stage, 2nd International Conference on the Behaviour of Materials, Boston, ZDA, 1976.

[2] Verreman, Y., Bailon, J-P., Masounave, J. Fatigue Life Prediction of Welded Joints A Re-assessment, Fatigue Fract. Engng. Mater. Struct.,10, 1, 17-36, 1987.

[3] Murakami, Y. at al. Quantitative Evaluation of Effects of Non-Metallic Inclusions on Fatigue Strength of High Strength Steels - I: Basic Fatigue Mechanism and Evaluation of Correlation between the Fatigue Fracture Stress and the Size and Location of Non-Metallic Inclusions, Int. J. of Fatigue, 9, 291-298, 1989.

[4] Murakami, Y., Usuki, H. Quantitative Evaluation of Effects of Non-Metallic Inclusions on Fatigue Strength of High Strength Steels - II: Fatigue Limit Evaluation Based on Statistics for Extreme Values of Inclusion Size, Int. J. of Fatigue, 9, 299-308, 1989.

[5] Murakami, Y. Effects of Small Defects and Nonmetallic Inclusions on Fatigue Strength of Metals, JSME International Journal I, 32, 2, 167-180, 1989.

[6] Gliha, V. Vpliv umetnih površinskih napak na dinamično trdnost materiala na prehodu temena vara. *Mater. tehnol.*, Vol. 35, 1/2, 55-59, 2001

[7] Gliha, V. The effect of small flaws on the fatigue strength of HAZ at the weld toe. *Int. j. mater. prod. technol.*, Vol. 29, 1/4, 297-310, 2007.

[8] Gliha, V. Vuherer, T. The Behaviour of Coarse-Grain HAZ Steel with Small Defects during Cyclic loading, Materials and Technology, 41, 3, 125-130, 2007.

[9] Vuherer, T. at al. Fatigue Crack Initiation from Microstructurally Small Vickers Indentations, Metalurgy, 46, 4, 237-243, 2007.

[10] Vuherer, T. Analysis of influence of micro defects on the fatigue strength of coarse grain HAZ in welds, Doctoral thesis, University of Maribor, Faculty for Mechanical Engineering, 2008.

[11] Peterson, R. E. Stress Concentration Factors, Wiley, 1974.
[12] Vuherer, T. Analiza zaostalih notranjih napetosti s posebnim povdarkom na ponovnem vnosu toplote in njih meritev v sočelnih zvarnih spojih, Master degree work, University of Maribor, Faculty for Mechanical Engineering, 1999.
[13] Miller, K. J. The Behaviour of Short Fatigue Cracks and Their Initiation Part I and Part II, Fatigue Fract. Engng. Mater. Struct., 10, 1, 75-91 and 2, 93-113, 1987.